SUPPORTING INFORMATION :

Reverse Iodine Transfer Polymerization (RITP) of Methyl Methacrylate

Cyrille Boyer, Patrick Lacroix-Desmazes, Jean-Jacques Robin, Bernard Boutevin*

UMR 5076 CNRS-ENSCM, Laboratoire de Chimie Macromoléculaire, Ecole Nationale Supérieure de Chimie de Montpellier, 8 rue de l'Ecole Normale. 34296 Montpellier Cedex 5, France.

cyrille.boyer@enscm.fr, patrick.lacroix-desmazes@enscm.fr, jrobin@univ-montp2.fr, bernard.boutevin@enscm.fr

Corresponding Author Footnote: UMR 5076 CNRS-ENSCM, Laboratoire de Chimie Macromoléculaire, Ecole Nationale Supérieure de Chimie de Montpellier, 8 rue de l'Ecole Normale. 34296 Montpellier Cedex 5, France. Tel. 33-4-67-14-72-05, fax : 33-4-67-14-72-20. patrick.lacroix-desmazes@enscm.fr

I. Evolution of [A-I] and [A-M_n-I] versus time, evolution of the iodine functionality of the polymer chains determined by ^{1}H-NMR spectroscopy during reverse iodine transfer polymerization of methyl methacrylate at 80°C in d^8-toluene.

To have a more precise knowledge of what happens during the inhibition period between the different species, the reaction was directly performed in a spectrometer and followed on line by ^{1}H NMR. It allowed us to determine the evolution of the monomer conversion (α) (Equation 1) and the concentration of the A-I adduct (Equation 2) versus time. According to Scheme 2 of the manuscript, $A^\bullet$ can react with iodine to give A-I, or initiate the polymerization of the monomer to form A-$M_n^\bullet$ oligoradicals which can also react with iodine to form A-M_n-I oligomers. It is possible to follow the appearance of these species by ^{1}H NMR. The various chemical shifts for the AIBN initiator, the recombination product A-A, and the adduct A-I were determined by ^{1}H NMR (Table 1) and a follow-up of the formation of A-I during RITP was carried out.

The monomer conversion (α) *versus* time was calculated by using the values of integration of the vinylic protons (CH_2=C(CH_3)CO_2CH_3) of methyl methacrylate at 5.30 ppm and at 5.95 ppm (Equation 1). The integral of the methoxy protons -OCH_3 (of monomer and polymer) is used as internal reference because its intensity does not vary versus time.

$$\alpha = 1\text{-}([MMA]_t/[MMA]_0) = 1 - ((\int^{5.30\&5.95ppm} CH_2{=}C/2)/(\int^{3.5ppm} \text{-}OCH_3/3)) \qquad \text{(Equation 1)}$$

in which $[MMA]_t$ and $[MMA]_0$ are the monomer concentrations at a given time *t* and at *t*=0, respectively.

As previously, an inhibition period is observed in agreement with the mechanism proposed in Scheme 2 of the manuscript. Moreover, it appears two stages: a first stage where the

monomer conversion is null and a second stage where there are a low monomer conversion and polymer formation (Figure 2 of the manuscript). The polymer formation is indicated by the change of aspect of the -OCH_3 signals at 3.50 ppm (one signal for the monomer and one signal for the polymer) and the appearance of a new signal towards 1 ppm assigned to the –C(CH_3) of the PMMA chains (shift from 1.80 ppm to 1.00 ppm). In parallel, we tried to follow the formation of the A-I adduct by ^{1}H NMR. The signal of the IC(CN)(CH_3)$_2$ (Table 1) appears towards 1.97 ppm near the signal of the -C(CH_3)- of MMA (1.80 ppm). In spite of their proximity, it is possible to follow the evolution of this signal versus time. As previously, the integral of the methoxy protons (-OCH_3) (at 3.50 ppm) was taken as internal reference (constant intensity versus time). Thus, it is possible to calculate the concentration of A-I, [A-I]$_t$, by using Equation 2.

$$[\text{A-I}]_t = [\text{MMA}]_0 \times (\int^{1.97\text{ppm}} \text{IC(CN)(C}H_3)_2/6)/(\int^{3.5\text{ppm}} \text{-OC}H_3/3) \qquad \text{(Equation 2)}$$

As in the case of RITP of methyl acrylate[1], two stages can be distinguished during the inhibition period (Figure 2 of the manuscript): appearance and disappearance of the A-I adduct.

Table 1. Assignment of ^{1}H NMR peaks for 2,2'-azobisisobutyronitrile (AIBN), iodo-adduct (A-I), and coupling product (A-A) in d^{8} deuterated toluene at 80°C.

Structures	Abbreviations	Chemical shifts in ppm (given in d^{8} toluene) at 80 °C
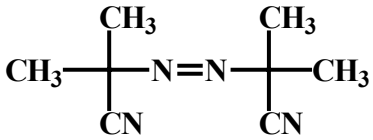	AIBN	1.46
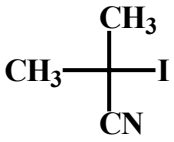	A-I	1.97
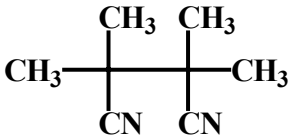	A-A	1.13

Figure 1 & Figure 2 below describe the evolution of $[A\text{-}I]_t$ (Equation 2) and $[A\text{-}M_n\text{-}I]_t$ (Equation 3) as well as the iodine functionality F^{iodine} of the polymer chains (Equation 4) for a RITP experiment.

$$[A\text{-}M_n\text{-}I]_t = [MMA]_0 \times (\int^{2.80ppm}\text{-}CH_2CI(CH_3)(CO_2CH_3)/2)/(\int^{3.5ppm}\text{-}OCH_3/3) \qquad \text{(Equation 3)}$$

$$F^{iodine} = (\int^{2.80ppm}\text{-}CH_2CI(CH_3)(CO_2CH_3)/2)/(\int^{1.2ppm}\text{-}C(CN)(CH_3)_2/6) \qquad \text{(Equation 4)}$$

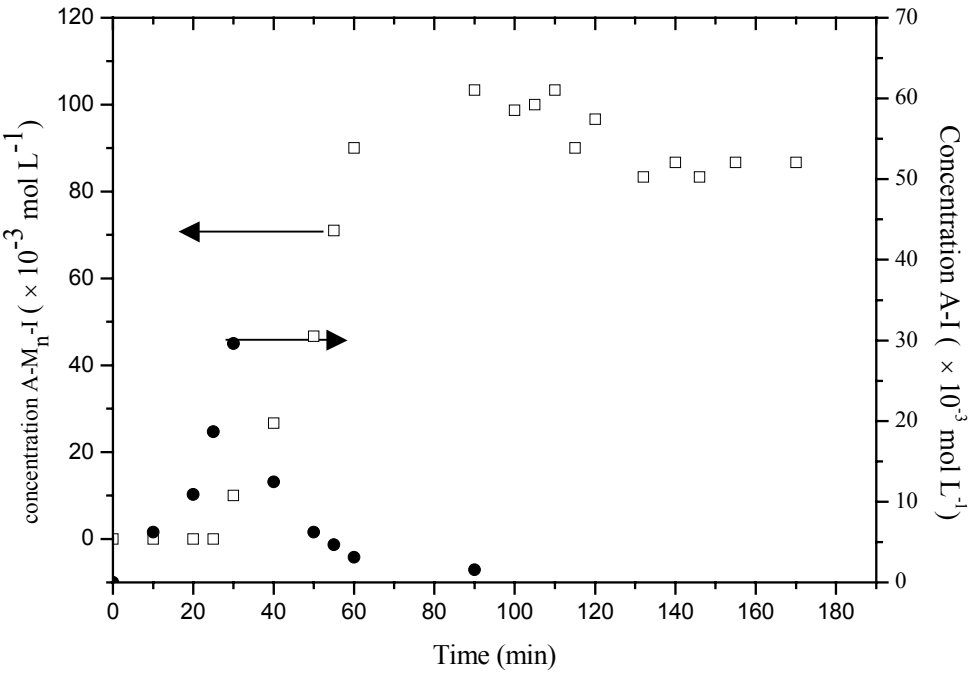

Figure 1. Evolution of $[A\text{-}I]_t$ (●) and $[A\text{-}M_n\text{-}I]_t$ (□) concentrations determined by ^{1}H NMR *vs* time.

Experimental conditions [MMA]/[AIBN]/[I_2] = 100/2.6/1: 5.000 g (5.00×10^{-2} mol) of methyl methacrylate (MMA), 0.213 g (1.30×10^{-3} mol) of 2,2'-azobisisobutyronitrile (AIBN), 0.128 g (5.04×10^{-4} mol) of iodine (I_2). 0.300 g of this solution was added with 0.20 g of deuterated toluene in the NMR tube.

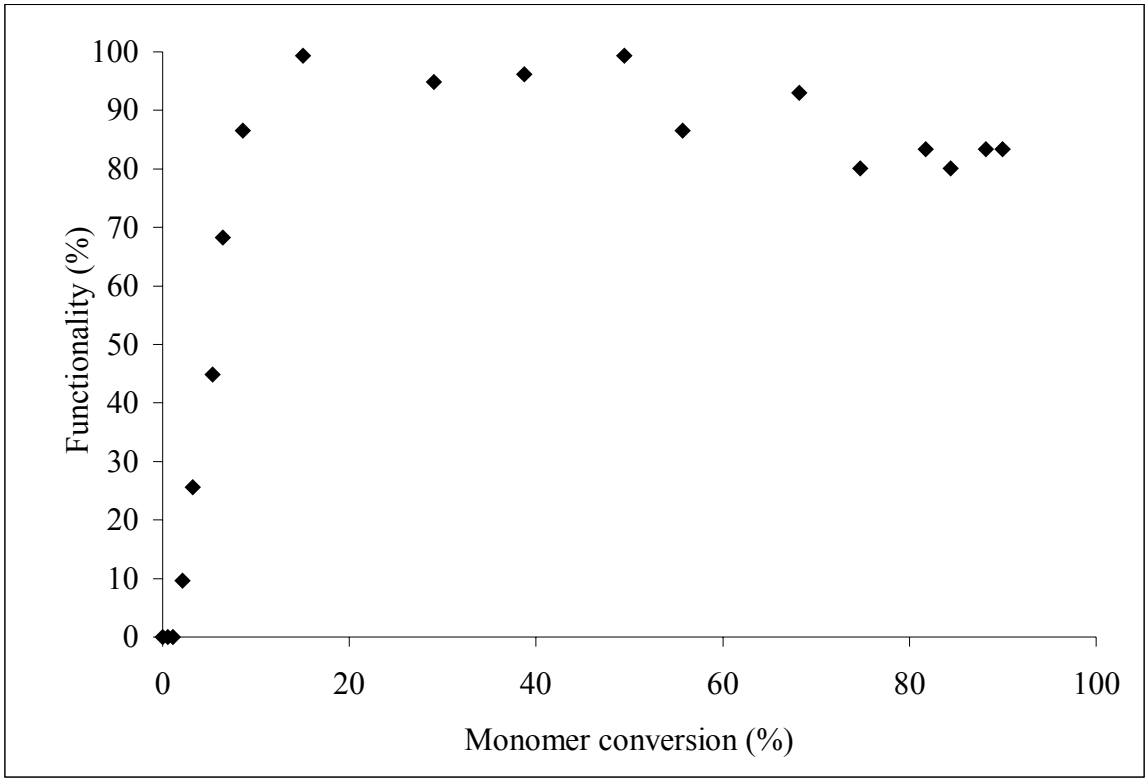

Figure 2: Evolution of the iodine functionality F^{iodine} of the polymer chains *vs* conversion.

Experimental conditions [MMA]/[AIBN]/[I_2] = 100/2.6/1: 5.000 g (5.00×10^{-2} mol) of MMA, 0.213 g (1.30×10^{-3} mol) of AIBN, 0.128 g (5.04×10^{-4} mol) of iodine (I_2). 0.300 g of this solution was added with 0.20 g of deuterated toluene in the NMR tube.

II. Evolution of Ln([M]$_0$/[M]) versus (1-exp(-$k_d \times \tau$ /2)) for reverse iodine transfer polymerizations of methyl methacrylate performed with [AIBN]=0.25M (Figure 3), 0.20M (Figure 4) and 0.17M (Figure 5) at 80°C, and summary of $k_p/k_{te}^{1/2}$ values (Table 2).

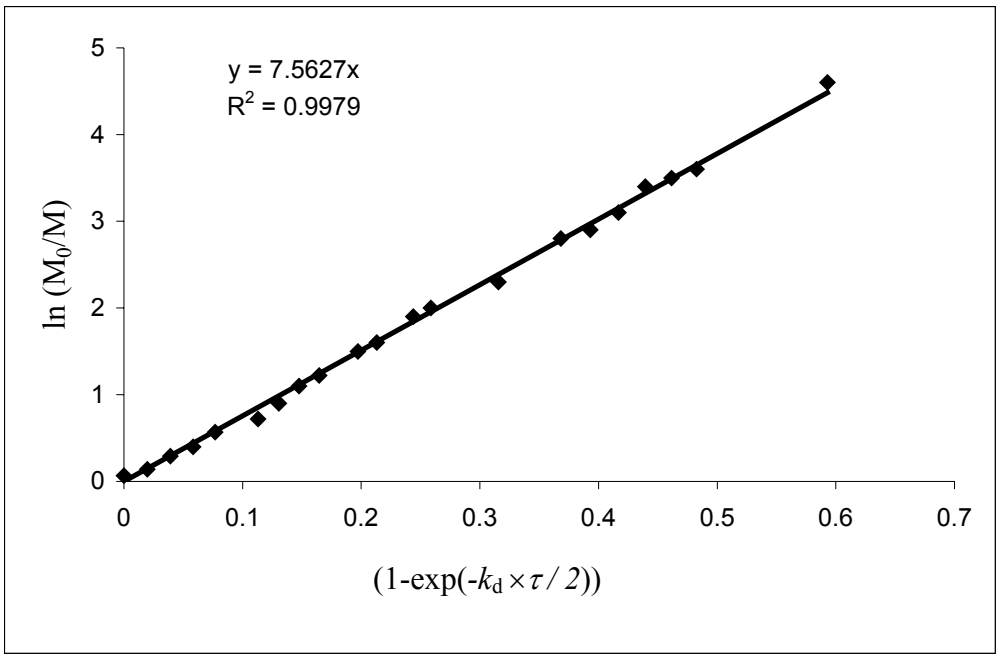

Figure 3. Evolution of ln (M_0/M) vs (1-exp(-$k_d \times \tau / 2$)) for RITP of MMA performed with [AIBN] = 0.25 M at 80°C.

Experimental conditions [MMA]/[AIBN]/[I_2] = 50/2.6/1:
25.00 g (2.5×10^{-1} mol) of MMA, 2.12 g (1.29×10^{-2} mol) of AIBN, 1.27 g (5.0×10^{-3} mol) of iodine (I_2) and 25 mL of toluene.

Determination of $k_p/k_{te}^{1/2}$:

Time inhibition = 75 min.
$[AIBN]_0 = 0.25$ M
$[AIBN]_{t,\ inh.} = 0.137$ M
$\ln([M]_0/[M]_t) = 2\ k_p \times (f \times [AIBN]_{t,inh})^{1/2}/(k_d \times k_t)^{1/2} \times (1\text{-}\exp(-k_d \times \tau / 2))$,
with $k_d = 1.331 \times 10^{-4} s^{-1}$, $f = 0.7$, $\tau = (t\text{-}t^{inh})$

Value of $k_p/k_{te}^{1/2} = 0.141\ L^{1/2}\ mol^{-1/2}\ s^{-1/2}$

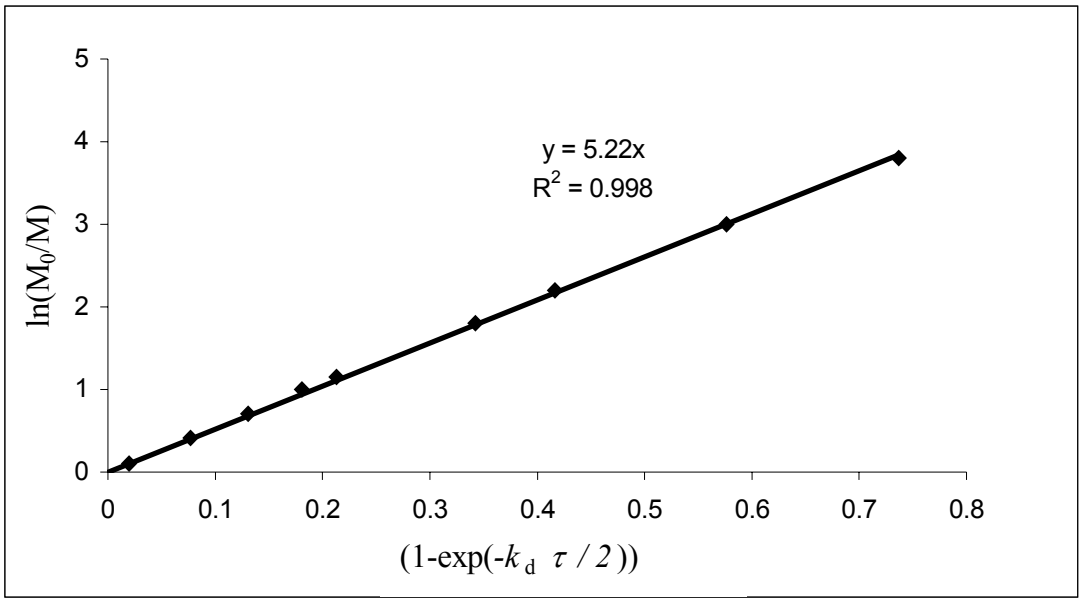

Figure 4. Evolution of ln (M_0/M) vs (1-exp(-$k_d \times \tau / 2$)) for RITP of MMA performed with [AIBN] = 0.20 M at 80°C.

Experimental conditions [MMA]/[AIBN]/[I_2] = 50/2.0/1:
25.00 g (2.5×10^{-1} mol) of MMA, 1.64 g (1.00×10^{-2} mol) of AIBN, 1.27 g (5.0×10^{-3} mol) of iodine (I_2) and 25 mL of toluene.

Determination of $k_p/k_{te}^{1/2}$:

Time inhibition = 166 min.
$[AIBN]_0$ = 0.20 M
$[AIBN]_{t,\ inh.}$ = 0.05 M
$\ln([M]_0/[M]_t) = 2\ k_p \times (f \times [AIBN]_{t,inh})^{1/2}/(k_d \times k_t)^{1/2} \times (1\text{-}\exp(-k_d \times \tau / 2))$,
with $k_d = 1.331 \times 10^{-4} s^{-1}$, $f = 0.7$, $\tau = (t\text{-}t^{inh})$

Value of $k_p/k_{te}^{1/2} = 0.161\ L^{1/2}\ mol^{-1/2}\ s^{-1/2}$

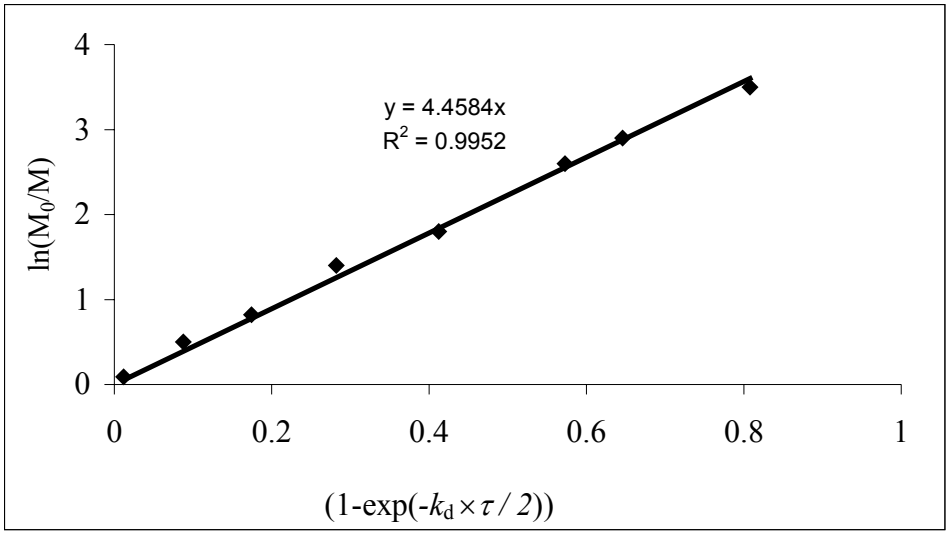

Figure 5. Evolution of ln (M_0/M) *vs* (1-exp(-$k_d \times \tau / 2$)) for RITP of MMA performed with [AIBN] = 0.17 M at 80°C.

Experimental conditions [MMA]/[AIBN]/[I_2] = 50/1.7/1:
25.00 g (2.5×10^{-1} mol) of MMA, 1.39 g (8.50×10^{-3} mol) of AIBN, 1.27 g (5.0×10^{-3} mol) of iodine (I_2) and 25 mL of toluene.

Determination of $k_p/k_{te}^{1/2}$:

Time inhibition (t^{inh}) = 240 min.
$[AIBN]_0$ = 0.170 M
$[AIBN]_{t,\ inh.}$ = 0.025 M
$\ln([M]_0/[M]_t) = 2\ k_p \times (f \times [AIBN]_{t,inh})^{1/2}/(k_d \times k_t)^{1/2} \times (1\text{-}\exp(-k_d \times \tau / 2))$,
with $k_d = 1.331 \times 10^{-4} s^{-1}$, $f = 0.7$, $\tau = (t - t^{inh})$

Value of $k_p/k_{te}^{1/2} = 0.194\ L^{1/2}\ mol^{-1/2}\ s^{-1/2}$

[AIBN] (mol L^{-1})	0.25	0.20	0.17
$k_p/k_{te}^{1/2}$ ($L^{1/2}\ mol^{-1/2}\ s^{-1/2}$)	0.141	0.161	0.194

Table 2. Summary of values $k_p/k_{te}^{1/2}$ ($L^{1/2}\ mol^{-1/2}\ s^{-1/2}$) for RITP of MMA performed at different concentrations of initiator (AIBN) at 80°C.

III. Characterization of a low molecular weight PMMA-I (M_n= 2 300 g mol^{-1}, M_w/M_n=1.4) by ^{13}C-NMR (Figure 6), elemental analysis (Equation 5), and assessment of the theoretical iodine functionality F^{iodine} (Equation 6).

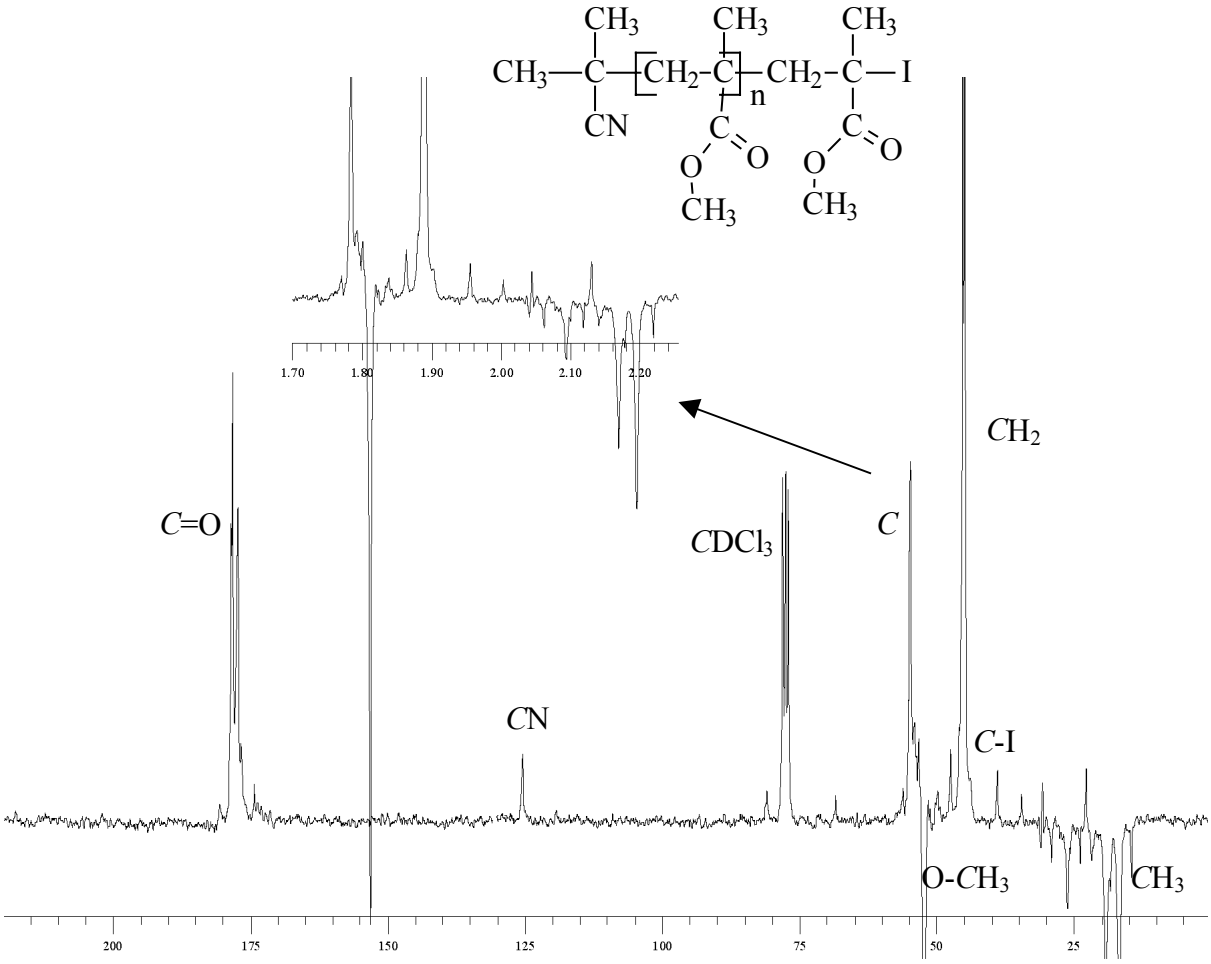

Figure 6. ^{13}C NMR spectrum of a low molecular weight PMMA-I (M_n = 2 300 g mol^{-1}, M_w/M_n = 1.4) in $CDCl_3$ (400 MHz).

This polymer (M_n = 2 300 g mol^{-1}, $DP_{n,SEC}$ = 21) was also analyzed by elemental analysis and the experimental values of 56.50% carbon, 27.80% oxygen, 7.60% hydrogen, 5.42% iodine, and 0.90% nitrogen, are close to the theoretical values of 57.00% carbon, 29.20% oxygen, 7.60% hydrogen, 5.50% iodine, and 0.60% nitrogen. Iodine can be in three different

forms in the sample: molecular iodine (I_2), hydriodic acid (HI), or at the polymer chain-end (C-I).

The proportion of free iodine atom (i.e. iodine atom which is not linked to the polymer chains) was determined by two methods:

(i) volumetric analysis with thiols (titration of iodine I_2);

(ii) ionic chromatography in liquid phase (titration of iodine I_2 and hydriodic acid HI).

In the first case, the percentage of free iodine is less than 0.1 wt%, and in the second case, it is around 996 ppm. The negligible quantity of HI in the polymer sample is consistent with the ^{1}H and ^{13}C NMR analyses which show the absence of double bond (no elimination of HI). From these results, it is possible to evaluate the iodine functionality F^{iodine}(Equation 5).

$$F^{iodine}=(wt\%_{iodine,total} - wt\%_{iodine,free})/(wt\%_{iodine,theoretical}) \qquad \text{(Equation 5)}$$

in which $wt\%_{iodine,total}$ is the total percentage of iodine in the sample, $wt\%_{iodine,free}$ is the percentage of free iodine in the sample (traces of HI and I_2), and $wt\%_{iodine,theoretical}$ is the theoretical percentage of iodine in the sample, calculated by $wt\%_{iodine,theoretical} = M^{iodine\ atom} \times 100/M_n$, in which $M^{iodine\ atom}$ = 127 g $mol^{-1}$and M_n is the mean number average molecular weight of the sample.

The experimental values of F^{iodine} should be compared to the theoretical iodine functionality, F^{iodine} (theoretical), given by equation 6.

$$F^{iodine}\,(\text{theoretical}) = 2\times[I_2]_0/(2\times[I_2]_0 + 2f\times\Delta\text{AIBN}) \qquad \text{(Equation 6)}$$

in which ΔAIBN is the excess amount of AIBN used to initiate and propagate the polymerization during the polymerization period ($\tau_{polym.}$) (after the inhibition period).

The value of ΔAIBN is evaluated by $\Delta AIBN = [AIBN]_{t,\,inh} \times (1 - \exp(-k_d \times \tau_{polym.}))$, with $\tau = (t - t^{inh})$. As an example, for the sample of M_n = 2 300 g mol^{-1} (monomer conversion ≈ 70%) synthesized with $[AIBN]_0/[I_2]_0 = 1.7$ and $[I_2]_0 = 0.074$ mol L^{-1}, the inhibition time is t^{inh}=240 min ($[AIBN]_{t,inh} = 0.018$ mol L^{-1}, with $k_d = 1.331 \times 10^{-4}$ s^{-1} at 80 °C for AIBN[2]), and the polymerization time is τ_{polym}= 60 min (ΔAIBN = 0.007 mol L^{-1}) leading to the theoretical iodine functionality F^{iodine}= 94%. The experimental values of F^{iodine} (about 95%) determined by the different methods (^{1}H NMR, ^{13}C NMR, and elemental analysis) are in good agreement with the calculated theoretical value (94%) (Table 3 of the manuscript).

IV. Characterization of a low molecular weight PMMA-I (M_n= 2 300 g mol^{-1}, M_w/M_n=1.4) by MALDI-TOF (Figure 7) (Table 3).

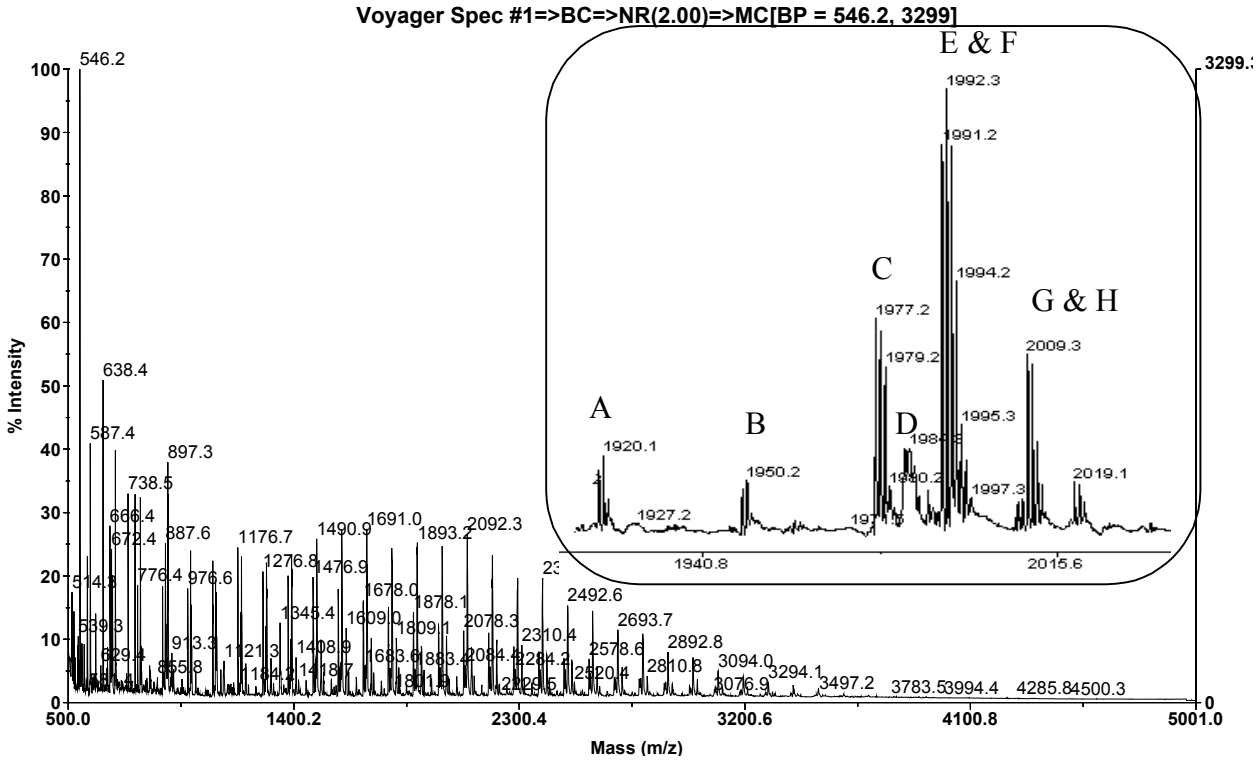

Figure 7. Mass-assisted laser desorption ionization time-of-flight (MALDI-TOF) analysis of a low molecular weight poly(methyl methacrylate) prepared by Reverse Iodine Transfer Polymerization of methyl methacrylate (MMA) at 80°C in toluene initiated by 2,2'-azobisbutyronitrile (AIBN) in the presence of iodine (I_2) with [MMA]/[AIBN]/[I_2]=60/1.7/1 (monomer conversion= 70%, M_n = 2 300g mol^{-1}, M_w/M_n = 1.4) (Inset is an expanded spectrum showing several polymer series).

The chromatogram (Figure 7) shows a series of peaks separated by *m/z*=100 (corresponding to the molecular weight of the MMA monomer unit). By focusing on the zone from *m/z* = 1915 to 2030, eight different series (A, B, C, D, E, F, G, H) are distinguished and the possible corresponding structures are given in Table 3.

The expected A-M_n-I structure appears at *m/z* = 1919.01 with a weak intensity (Table 3, series A).

The distribution at *m/z* = 1977.23 can be ascribed to the elimination of CH_3I from the A-M_n-I polymer chains (lactone formation, Scheme 3 of the manuscript) (Table 3, series C). This loss of CH_3I can be achieved at high temperature (150 °C) or during MALDI-TOF analysis. This is consistent with various studies reported in the literature (polymers of PMMA terminated by a bromine atom[3] or by a chlorine atom[4-6]).

The distribution at *m/z* = 1991.24 can be attributed to the vinyl terminated PMMA chains (Table 3, series E) (note: the distribution at *m/z* = 2008.23 corresponds to the same structure cationized with K^+, Table 3, series G). These unsaturared chains might arise from termination by disproportionation (Scheme 1). The corresponding saturated polymer chains (A-M_n-H structure, cationized with Na^+) would correspond to the signal at *m/z*=1993.25 (Table 5, series F) (the distribution at *m/z*=2009.25 corresponds to the same structure cationized with K^+, Table 3, series H). However, since no double bond is detected by ^1H and ^{13}C NMR, it is thought that the distribution at *m/z* = 1991.24 mainly comes from the elimination of HI from A-M_n-I polymer chains during the MALDI-TOF analysis (Scheme 3 of the manuscript). In the literature, this case was already observed for methacrylate or acrylate oligomers terminated by chlorine or bromine atoms[5,7]. Nonaka et al.[7] showed that this reaction of elimination of HCl for the PMMA-Cl is carried out during the laser irradiation. According to the power of the laser, the deshydrohalogenation is more or less significant.

The distributions with a weak intensity at *m/z* = 1983.47 (Table 3, series D) and at *m/z* = 1949.23 (Table 3, series B) could not be attributed.

In conclusion, the MALDI-TOF analysis is not sufficient to characterize the structure of the polymer chains because they undergo significant modifications during the analysis (elimination of CH_3I, elimination of HI).

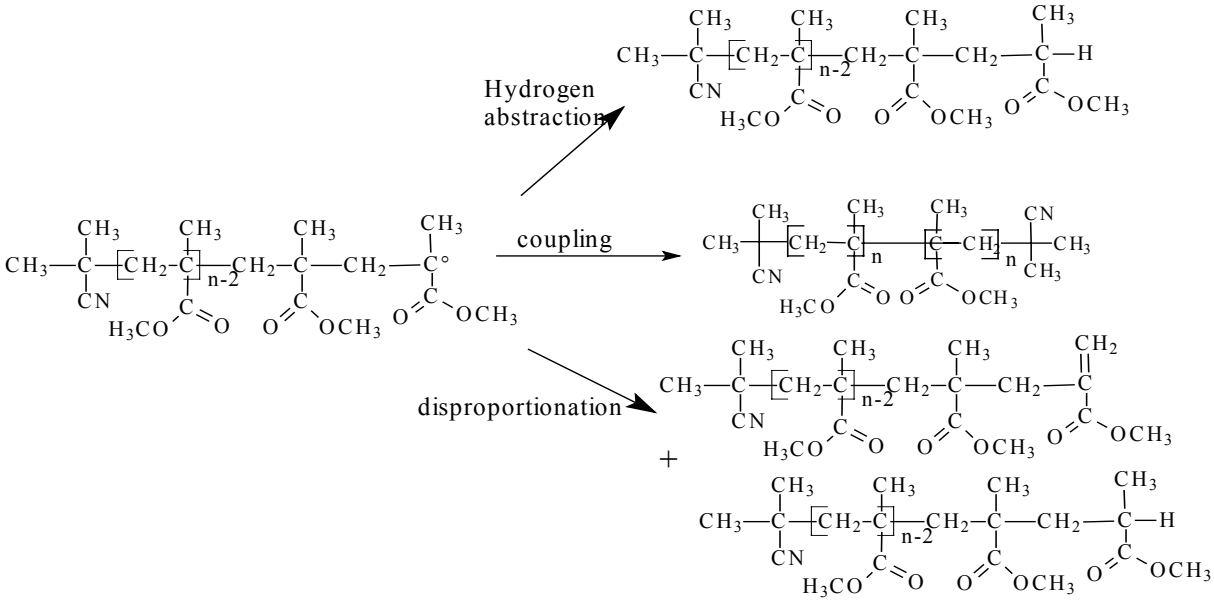

Scheme 1. Formation of dead chains in radical polymerization of methyl methacrylate.

Table 3. Tentative assignment of peaks in the MALDI-TOF spectrum of a poly(methyl methacrylate sample (M_n = 2 300 g mol^{-1}, M_w/M_n =1.4) synthesized by Reverse Iodine Transfer Polymerization.

Series	*m/z* experimental	*m/z* theoretical monoisotopic mass	*n*	Structures
A	1 919.01	1 918.83	17	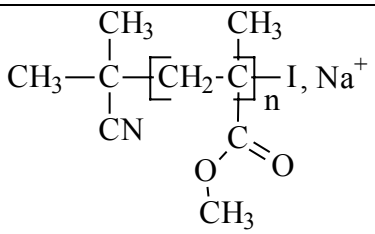
B	1949.23	-	-	Not attributed
C	1 977.23	1 977.01	19	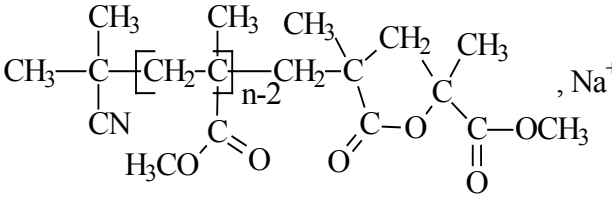
D	1 983.47	-	-	Not attributed
E	1 991.24	1 991.02	19	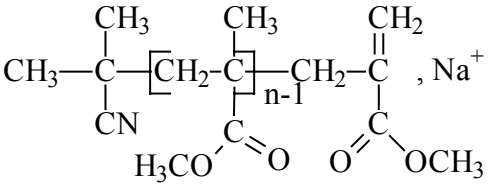
F	1 993.25	1 993.04	19	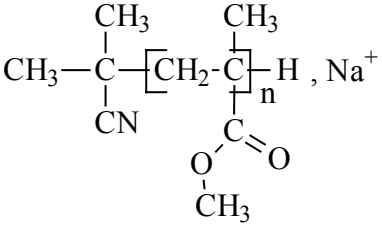
G	2008.23	2007.00	19	Idem series E, cationized K^+
H	2 009.25	2 009.01	19	Idem series F, cationized K^+

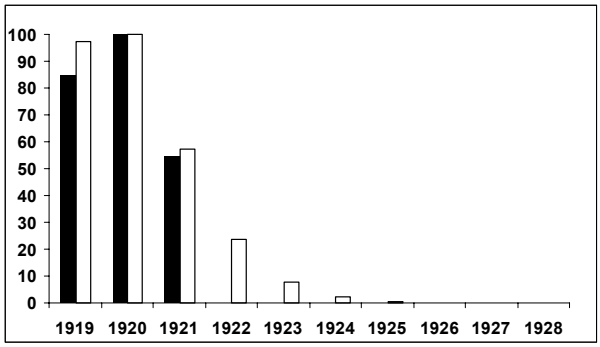

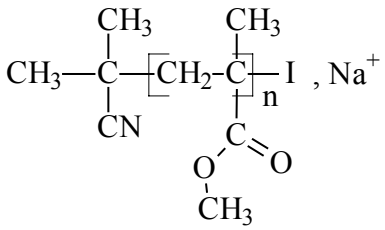

a- PMMA-I (*n*=17) (series A).

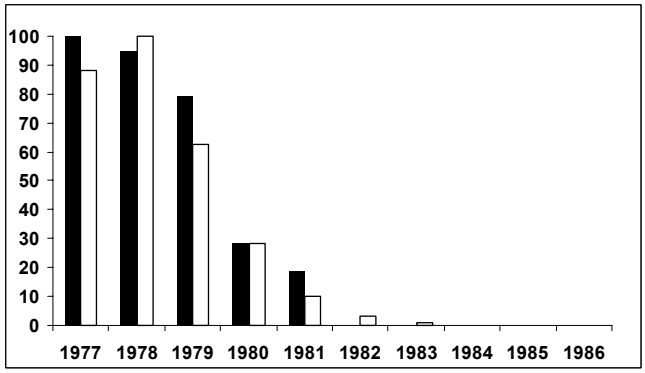

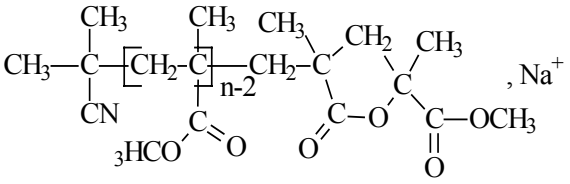

b- CH_3I elimination (*n*=19) (series B).

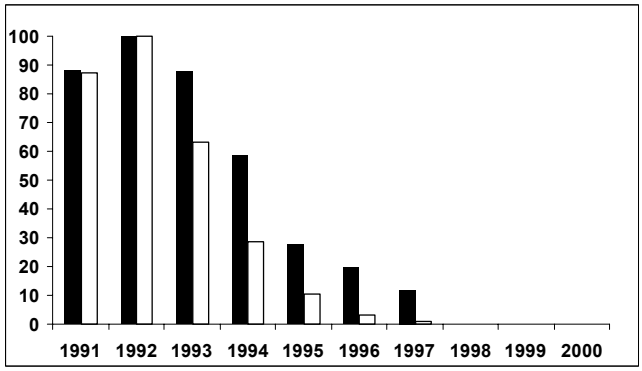

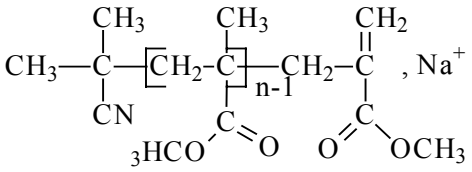

c- HI elimination or dismutation (*n*= 19) (series E).

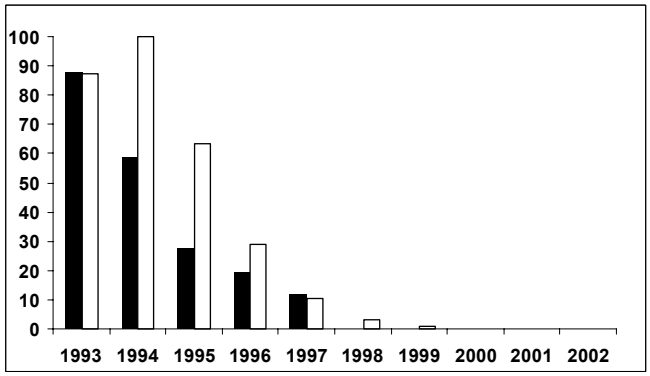

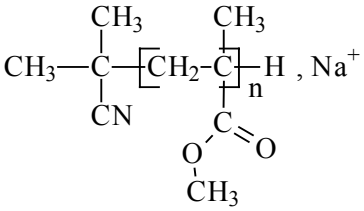

d- Transfer reaction to solvent or dismutation (PMMA-H) (*n*=19) (series F).

Figure 8. Simulated (white) and experimental (black) MALDI-TOF distributions for various possible structures.

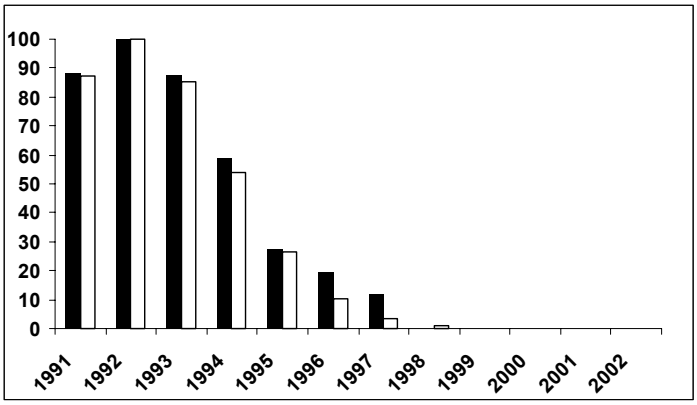

Figure 9. Simulated (white) and experimental (black) MALDI-TOF distributions for a linear combination of Series E & F (80/20).

REFERENCES:

(1) Lacroix-Desmazes, P.; Severac, R.; Boutevin, B. *Macromolecules* **2005**, *38*, 6299-6309.

(2) Van Hook, J. P.; Tobolsky, A. V. *J. Am. Chem. Soc.* **1958**, *80*, 779-782.

(3) McEwen, C. N.; Peacock, P. M.; Guan, Z. In *Proceding of the 45th ASMS conference on Mass Spectrometry and Allied Topics*, 1997, June 1-5; p 409.

(4) Jackson, A. T.; Yates, H. T.; Scrivens, J. H.; R., G. M.; H., B. R. *J. Am. Soc. Mass Spectrom* **1997**, *8*, 1206-1213.

(5) Coca, S.; Jasieczek, C. B.; Beers, K. L.; Matyjaszewski, K. *J. Polym. Sci. Part A; Polym. Chem.* **1998**, *36*, 1417-1424.

(6) Borman, C. D.; Jackson, A. T.; Bunn, A.; Cutter, A. L.; Irvine, D. J. *Polymer* **2000**, *41*, 6015-6020.

(7) Nonaka, H.; Ouchi, M.; Kamingaito, M.; Sawamoto, M. *Macromolecules* **2001**, *34*, 2083-2088.